ORIGINAL ARTICLE

IL-4 administration exerts preventive effects via suppression of underlying inflammation and TNF-α-induced apoptosis in steroid-induced osteonecrosis

X. Wu[1] · X. Feng[1] · Y. He[1] · Y. Gao[1] · S. Yang[1] · Z. Shao[1] ·
C. Yang[1] · H. Wang[1] · Z. Ye[1]

Abstract

Summary Macrophages play an important role during the development of steroid-induced osteonecrosis. Interleukin (IL)-4 administration helped reduce the infiltration of M1 phenotypic macrophages and maintain the activation of M2 phenotypic macrophages, resulting in restriction of inflammation and decrease in osteocyte apoptosis. The results indicated the therapeutic potential of IL-4 in prevention of steroid-induced osteonecrosis.

Introduction Steroid-induced osteonecrosis (ON) is a debilitating disease characterized by the activation and infiltration of macrophages into the necrotic site. This study aimed to investigate the effects of IL-4 administration on macrophage polarization and the involved signaling pathways.

Methods Fifty-six BALB/c mice were randomly divided into two groups, group M (model group) and group MI (treatment group), each containing 28 mice. ON model was induced by the injection of methylprednisolone (MPS). The mice in group MI received intra-abdominal injections of 2 μg/100 g/day of rIL-4 for five consecutive days, following the administration of MPS. Osteonecrosis was verified by histopathological staining. The expression of tumor necrosis factor-alpha (TNF-α) was analyzed by ELISA and immunohistochemistry. The infiltration of M1/M2 macrophages was examined by the expression of specific makers of F4/80, CD11c, and CD206 protein. Cell apoptosis was detected by terminal deoxynucleotidyl transferase-mediated dUTP nick end labeling (TUNEL) assay, and the apoptotic signal molecules such as STAT1 and caspase-3 were examined.

Results Histopathological observations indicated that IL-4 administration reduced the incidence of ON and the accumulation of osteoclasts. IL-4 administration inhibited the expression of TNF-α and reduced the infiltration of M1 phenotypic macrophages and maintained relatively high level of M2 phenotypic macrophages. Additionally, TUNEL assay suggested that IL-4 intervention could reduce the number of apoptotic cells in the necrotic zone. The anti-apoptotic mechanisms were related to STAT1 phosphorylation and the activation of caspase-3.

Conclusions Il-4 administration could alleviate steroid associated ON in mice by inhibiting the inflammatory response, the infiltration of M1 phenotypic macrophages, and suppressing TNF-a-induced osteocytic apoptosis by inhibiting the STAT1-caspase-3 signal pathway.

Keywords Apoptosis · IL-4 · Macrophages · Osteonecrosis · TNF-α

✉ H. Wang
wanghwh@126.com

✉ Z. Ye
56138779@qq.com

[1] Department of Orthopaedics, Union Hospital, Tongji Medical College, Huazhong University of Science and Technology, Wuhan 430022, China

Introduction

Non-traumatic osteonecrosis (ON), also known as avascular necrosis, is a common complication of corticosteroid treatment. The pathogenesis of ON is very complicated and cannot be explained by using a single theory. Based on the reported human and animal studies, several possible factors have been found in the pathogenesis of ON, including coagulation abnormalities, hyperlipidemia, oxidative stress, and vasospasm [1–3]. Unfortunately, the precise etiology of ON remains unclear and requires elucidation.

Macrophages, which are a population of cells derived from the bone marrow, infiltrate into tissues and become resident

tissue macrophages. Under certain circumstances, macrophages are activated to distinct phenotypes (M1 and M2 type) and play important roles in both disease and homeostasis within the tissues where they reside [4]. M1 macrophages play an important role in the removal of microorganisms and increase of pro-inflammatory cytokines, reactive nitrogen, and oxygen intermediates, whereas M2 macrophages are able to resolve inflammation, phagocytose apoptotic cells, inhibit the secretion of pro-inflammatory cytokines, and promote tissue remodeling, angiogenesis, and wound repair [5–7]. Alternative activation of macrophages (M2) is induced in the Janus protein kinase (JAK)-signal transducer and activator of transcription (STAT) pathway mediated by interleukin (IL)-4. After binding to IL-4Ra on the surface of macrophages, IL-4 induces phosphorylation of STAT6. IL-4 then forms a dimer, migrates, and binds to promoters of M2 genes to induce transcription in a STAT6-dependent manner [8, 9].

Recent studies have demonstrated the functional alterations in macrophages involved in several diseases, such as atherosclerosis, myocardial infarction, and skeletal muscle injury [10–12]. Macrophages are differentially activated during the development of myocardial infarction, with the presence of M1 macrophages in the ischemic phase, whereas the reparative phase is characterized by the presence of anti-inflammatory and reparative M2 macrophages [12, 13]. Muscular dystrophy is a disease related to the aberrant polarization of M1/M2 macrophages, with no observed M1 to M2 phenotypic shift, resulting in a failure to promote progenitor cell differentiation [14]. Another example of dysregulation of macrophage polarization is spinal cord injury (SCI), where a constant M1-predominant macrophage phenotype is observed with no shift to a resolving M2 phenotype at the lesion site, as seen in normal tissue repair [15]. Although the underlying mechanisms remain poorly understood, studies have demonstrated that the dysregulation of macrophage polarization and failure to restore M1/M2 macrophages to a normal balance are factors responsible for the chronic inflammatory process in injuries and disease states [16, 17]. However, this is not a unique instance, our previous results indicate that macrophages play key roles in the pathogenesis of steroid-induced osteonecrosis, dominated by pro-inflammatory M1 macrophages rather than anti-inflammatory M2 macrophages [18]. The balance between M1 and M2 macrophage activation is vital in the development of steroid-induced osteonecrosis, and an imbalance in the polarization of macrophage populations may be either detrimental or beneficial to ON progression.

Apparently, macrophages play an important role in the development and progression of steroid-induced osteonecrosis; however, the functional mechanism has not yet been elucidated. If the polar induction of macrophages can be controlled, the pathogenic process of ON could be altered and overturned. Thus, polarized macrophages and the involved signaling pathways are attractive targets for therapeutic strategies.

Materials and methods

All experiments were conducted in accordance with the Guidelines for Animal Experiments of Tongji Medical College.

Animal grouping

Sixty-two BALB/c mice with an average age of 8.5 weeks (range, 8–10 weeks) were used in the present study at the Experimental Animal Center of Tongji Medical College, HUST. The animals received a standard laboratory diet and water ad libitum. Fifty-six mice were divided randomly into two groups: group M (model group) and group MI (treatment group) ($n = 28$ each), the other six mice were housed as control group (CON). The murine ON model was established according to the reported protocols [19]. Briefly, the steroid-induced ON model was induced by one injection into the right gluteal muscle with 20 mg/kg of methylprednisolone (MPS; Pfizer, USA). ON gradually developed and was confirmed. In group MI, the mice received intra-abdominal injections of 2 μg/100 g/day of rIL-4 (Sigma-Aldrich, USA) for five consecutive days, following the administration of MPS. Six mice in the CON group received neither MPS nor rIL-4 treatment. No mice died in the groups throughout the experimental period.

Tissue sample preparation

The animals were sacrificed at 2 ($n = 8$) and 4 weeks ($n = 20$) after the last treatment for groups M and group MI, respectively ($n = 8$ vs. $n = 20$ in each group, respectively). Blood sample was collected from the inferior vena cava at the time of sacrifice and centrifuged immediately. The supernatant was stored at −80 °C until analysis. The proximal and distal femur and humerus were harvested from each mouse, half of each humerus was stored at −20, and the other half was fixed in 10 % formalin for 1 week and then decalcified in EDTA for 4 weeks. Next, the specimens were embedded in paraffin and cut into 4-μm sections for histopathological and immunohistochemical analysis.

ELISA assay

TNF-α is typically produced by macrophages, which exist widely in the area of inflammatory bone erosion. The level of TNF-α in blood samples was detected by ELISA according to manufacturer's procedures and using the stored blood supernatant from each group.

Histopathological staining

Histological analysis was performed by hematoxylin and eosin staining to observe the osteonecrotic changes in each group at different time points. For each group, the frequency of ON and its histology were examined. Whole areas of the proximal and distal ends of both femora and humeri were histopathologically examined for the presence of ON. In addition, the ratio of empty lacunae (empty lacunae/the total number of osteocytes) and the size of bone marrow fat cells were calculated. The histological sections were digitized into a microscope imaging system for quantification using image analysis software (HPIAS-1000) and subjected to a blinded analysis.

Tartrate-resistant acid phosphatase (TRAP) is a glycosylated monomeric metalloprotein enzyme that is highly expressed by osteoclasts, which are activated macrophages, under normal circumstances. Series of the sections from each group were stained with TRAP to determine osteoclast number during the progression of steroid-induced ON. For TRAP staining, hexazotized pararosanilin and naphthol ASTR phosphate (Sigma) were used to reveal osteoclasts, whereas tartaric acid was used to inhibit the non-osteoclastic acid phosphatase.

Immunohistochemical assessment

For immunohistochemical analysis, bone tissue sections were sampled form the whole tissue sections. After the sections were deparaffinized and rehydrated, antigen retrieval was performed by boiling the sections in citrate buffer for 15 min. Sections were then treated with 3 % hydrogen peroxide to inhibit endogenous peroxidase activity. After washing in TBS with 0.025 % Triton X-100, the sections were blocked with 5 % normal goat serum (Sigma-Aldrich) for nonspecific binding. After blocking, the sections were incubated overnight with one of the following primary antibodies: TNF-α (1:100; Bioss), F4/80 (1:50; abcam), and p-STAT1 (1:200; Santa Cruz Biotechnology). After washing, sections were incubated with peroxidase-labeled goat anti-mouse or anti-rabbit secondary antibodies (1:200; KPL) for 30 min at room temperature. Sections were then treated with diaminobenzidine (DAB) for 4 min and counterstained with hematoxylin-eosin for 10 min. The level of positive protein was observed through a microscope, and images were analyzed as the percentage of the total counterstained area with a computer-assisted image analysis system HPIAS-1000.

Immunofluorescence staining

For immunofluorescence staining, the sections were incubated in 5 % normal goat serum for blocking the nonspecific antibody binding. After blocking, the sections were incubated overnight with F4/80 (1:50; abcam), CD11c (1:100; abcam), CD206 (1:1000; abcam), caspase-3 (1:100; Sigma-Aldrich), or their mouse IgG isotype control mAbs. The secondary antibodies, goat anti-mouse fluorescein-conjugated antibodies (1:200, DAKO) or goat anti-rabbit fluorescein-conjugated antibodies (1:200, DAKO), were applied for 1 h at room temperature. In addition, the sections were counterstained with nuclear marker 4,6-diamino-2-phenylindole (DAPI). All images were obtained using a fluorescence microscope (Olympus). The percentage of M1 and M2 phenotype macrophages was calculated based on the positive staining observed in the cells.

Western blot analysis

Specimens from the left side of the animals were preserved at −70 °C for western blotting analysis. The frozen bone tissue was taken in a mortar with liquid nitrogen and crushed by mechanical disruption. Next, RIPA buffer (Cell Signaling Technology) was used for the extraction of the tissue's total protein; protein concentrations were measured using the Bio-Rad protein assay. Equalized protein samples were used for electrophoresis. After electrophoresis, the proteins were then electro-transferred to 0.45-μm pore-diameter polyvinylidene difluoride (PVDF) membranes (Invitrogen) and immunolabeled with caspase-3 (1:200; Sigma-Aldrich) and p-STAT1 (1:250; Santa Cruz Biotechnology) overnight at 4 °C. Then, the membranes were incubated for 2 h at 4 °C with a 1:2000 dilution of HRP-conjugated secondary antibody in antibody diluent. Finally, the ECL Plus western blotting system was used, and immunoreactive bands were revealed and quantified using ImageQuant LAS 400 software (GE Healthcare Life Sciences) and calculated by normalization to the reference bands of β-actin.

TUNEL assay

Apoptosis of the osteoblasts and osteocytes was assessed by the terminal deoxynucleotidyl transferase-mediated dUTP nick end labeling (TUNEL) assay. For TUNEL staining, paraffin sections from each group were stained with an In Situ Cell Death Detection Kit (Roche) after deparaffinizing, rehydrating, and washing, according to the manufacturer's instructions.

Statistical analysis

All data are expressed as mean ± SEM from at least three independent experiments. Statistical analyses were performed using Prism v. 5.0 (GraphPad Software, Inc.), and differences between groups were examined for statistical significance using one-way factorial analysis of variance (ANOVA) or t test. A p value <0.05 was considered to indicate a statistically significant result.

Results

IL-4 intervention reduces osteonecrotic changes in steroid-induced ON mice

The incidence rate of ON and the osteonecrotic process in mice in each group were histopathologically observed to evaluate the potential effects of Il-4 intervention on steroid-induced ON in mice. Figure 1a shows the histopathological characteristics of ON after HE staining at weeks 2 and 4 in groups M and group MI, respectively. In group M, at week 2, the presence of empty lacunae and pyknotic nuclei of osteocytes were found in the necrotic bone trabeculae; at week 4, numerous pyknotic nuclei and empty lacunae were observed in the necrotic bone trabeculae, with the entry of fibrous tissue in the medullary space. The incident rates of osteonecrosis in group M and group MI were 77.27 and 45 %, respectively. Compared with group M, the ratio of empty lacunae in group MI was significantly less at week 2 and week 4 (15.43 ± 5.41 vs. 24.6 ± 7.92 %, 24.63 ± 4.72 vs. 38.22 ± 7.65 %), respectively (Fig. 1c). In addition, adipocyte perimeters were similar in both groups at week 2 but were significantly smaller in group MI than in group M at week 4 (36.46 ± 4.98 vs. 52.7 ± 7.56 %) (Fig. 1d). There was no visible necrosis of bone or bone marrow in control group.

IL-4 administration decrease TRAP activity

Histomorphometric examination of the bone sections from different groups revealed that osteoclasts increased and accumulated in the necrotic zone during the progression of ON and resorbed the necrotic bone trabeculae. The mean osteoclast number was significantly higher in group M (6.9 ± 1.33 and 13.57 ± 3.49 mm^2) than in group MI (4.58 ± 1.43 and 9.69 ± 1.11 mm^2) and CON group (0.52 ± 0.20 and 0.51 ± 0.18 mm^2) at week 2 and week 4, respectively. In addition, similar results were found by testing TRAP activity in serum. It was found that the TRAP concentrations in group M were increased obviously during the progress of ON and were much higher than that in group MI (Fig. 2).

Decreased TNF-α expression after IL-4 intervention during ON

TNF-α plays an important role in the development of steroid-induced ON. The expression of TNF-α protein was detected by the immunohistochemical method using bone sections obtained from different groups. As shown in Fig. 3a, TNF-α protein expression was high at week 2 in group M, then got attenuated and maintained a relatively high level at week 4. Compared with group M, TNF-α
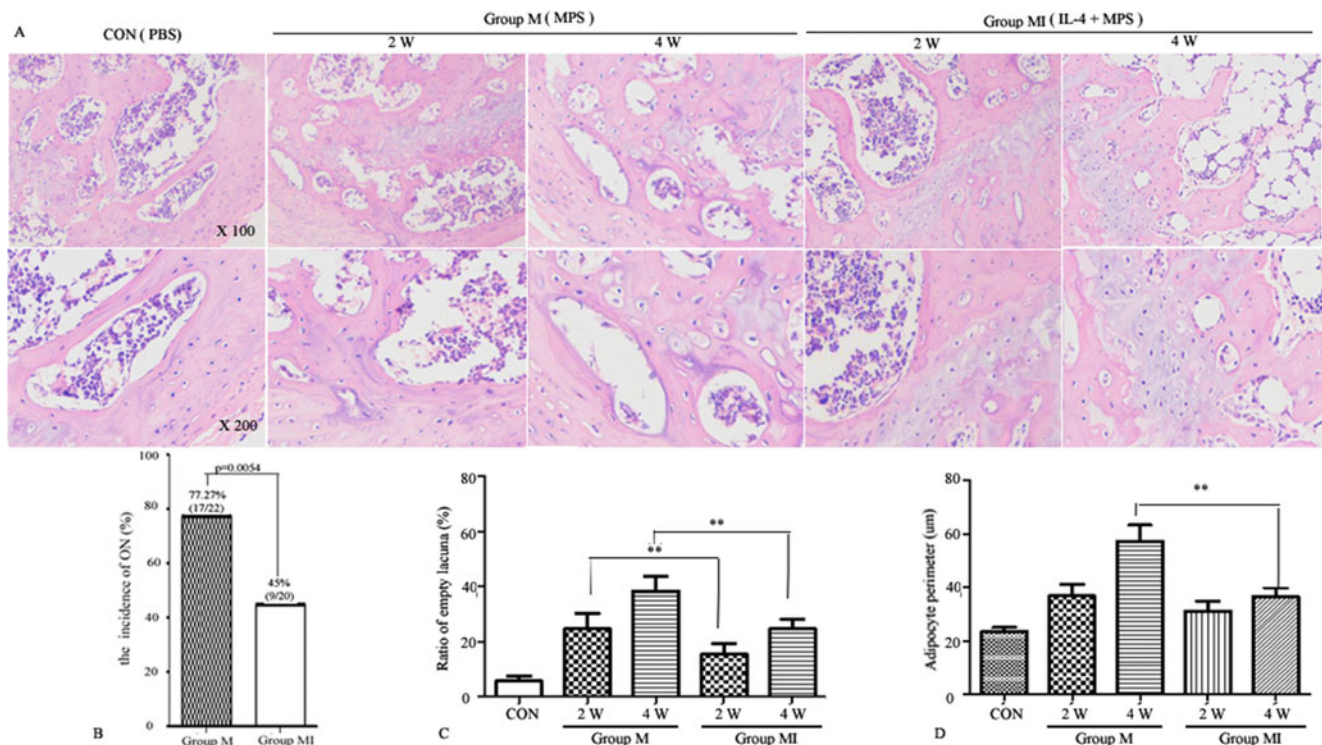

Fig. 1 Osteonecrosis as observed by hematoxylin-eosin staining in the two groups. **a** Histopathological changes of bone tissue in the CON, M, and MI groups (×100, ×200). **b** The incidence of ON was much higher in group M than in group MI. **c** Statistical analysis on the differences of the ratio of empty lacunae in both groups at weeks 2 and 4. **d** Statistical analysis on the differences of the adipocyte perimeter in the groups. Data are represented as the mean ± SD. **$P < 0.01$ compared with group M
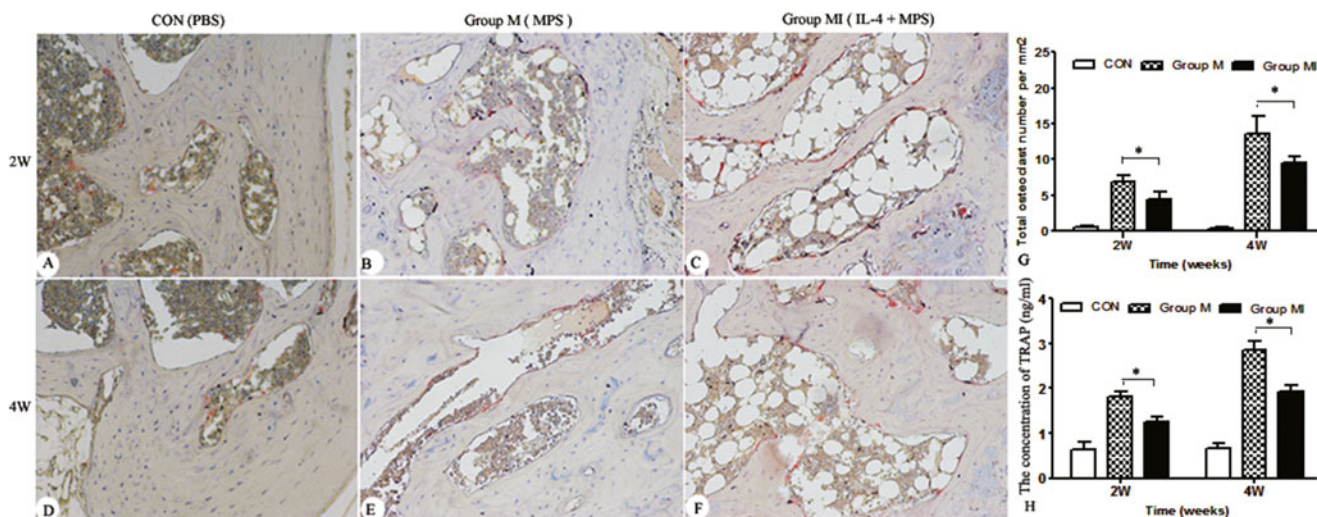
Fig. 2 Tartrate-resistant acid phosphatase (TRAP) activity during steroid-induced ON. **a–c** High-magnification photomicrographs of sections were stained with TRAP to visualize osteoclasts in CON (**a**), group M (**b**), and group MI (**c**) at week 2. **d–f** Photomicrographs for TRAP activity in CON (**d**), group M (**e**), and group MI (**f**) at week 4. **g**

Bar graph showing the mean number of osteoclasts in each group at different time points. **f** The serum concentrations of TRAP were tested by ELISA and analyzed statistically. Data showed the mean ± SEM. *$P < 0.05$ vs. group M

protein expression was much lower after IL-4 administration in group MI at weeks 2 and 4. Meanwhile, low levels of TNF-α were expressed in the CON group during the progression of ON. In addition, serum TNF-α level was measured by using ELISA, as shown in Fig. 3b. Serum TNF-α concentration was significantly higher in group M (75.06 ± 10.92 and 41.03 ± 6.49 pg/mL) than in group MI (55.83 ± 9.91 and 27.01 ± 4.12 pg/mL) and in the CON group (20.8 ± 6.46 and 21.1 ± 4.83 pg/mL) at weeks 2 and 4, respectively. These findings indicate that the accumulation of TNF-α during ON and IL-4 intervention could weaken the expression of TNF-α, which might be useful for inhibition of the local inflammatory response and the accompanying osteonecrosis.

IL-4-medicated M1/M2 macrophage alterations during ON

We detected the effects of IL-4 on the polarization and function of M1/M2 macrophages in vitro and explored the potential underlying mechanisms. For identifying M1 and M2 macrophages, specific markers for the M1 (CD 11c) and M2 phenotypes (CD206) were used, combined with the mutual specific marker (F4/80). The proteins of F4/80, CD11c, and CD206 expression were detected by immunofluorescence staining in the CON, group M, and group MI. Representative histological images of the three groups and the corresponding time points demonstrated that IL-4 treatment decreased F4/80+-stained macrophages, especially
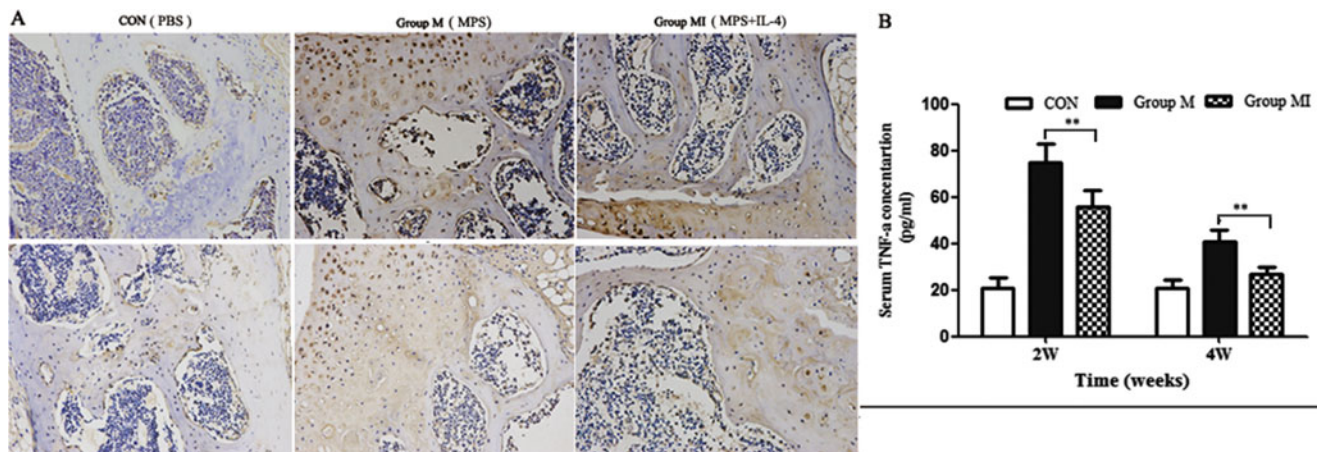

Fig. 3 The expression of TNF-α in different groups during ON. **a** The protein expression of TNF-α at different time points were measured by immunohistochemical method in the CON, M, and MI groups. **b**

Statistical diagram showed the serum TNF-α concentration in different groups. Data showed the mean ± SEM. **$P < 0.01$ vs. group M

at week 2. These images also indicated the simultaneous presence of both M1 (F4/80 + CD11c+) and M2 (F4/80 + CD206+) macrophages during ON, and IL-4 administration was shown to decrease M1 and M2 macrophages at weeks 2 and 4 (Fig. 4a). Quantification of the cell counts from the histological images indicated that MPS induction increased the accumulation of F4/80+-stained macrophages, whereas IL-4 treatment decreased the infiltration of F4/80+-stained macrophages (Fig. 4b). Similarly, MPS induction was shown to significantly increase the number of macrophages at weeks 2 and 4, whereas IL-4 treatment decreased the infiltration of both M1 (Fig. 4c) and M2 (Fig. 4d) macrophages. However, significant changes were not observed in the relative number of M2 macrophages after IL-4 administration at weeks 2 and 4, which might be beneficial for tissue regeneration and repair. The control treatment produced minimal F4/80+-, F4/80 + CD11c+-, and F4/80 + CD206+-stained macrophages. Thus, the results demonstrated that IL-4 administration could reduce the infiltration of M1 phenotypic macrophages and maintain a relatively high level of M2 phenotypic macrophages,

resulting in restriction of inflammation and acceleration of tissue repair.

IL-4 administration suppresses p-STAT1 signal pathway

The expression patterns and subchondral localization of p-STAT1 protein in the bone tissues of both the groups were detected by the immunohistochemical method. Positive immunoreactivity of p-STAT1 in each group was analyzed. Immunostaining for p-STAT1 increased significantly in group M at weeks 2 and 4; however, the increase was minor in group MI (Fig. 5a). We further detected the changes in p-STAT1 expression at the protein level in different groups with or without IL-4 administration in order to evaluate its influence on the pathway. Quantitative analysis demonstrated that compared with group MI, there was a significant increase in protein expression in group M at weeks 2 and 4 ($p < 0.01$) but not in the CON group (Fig. 5b, c). The results showed that the p-STAT1 signaling pathway was involved in steroid-induced ON, which could be controlled by IL-4.
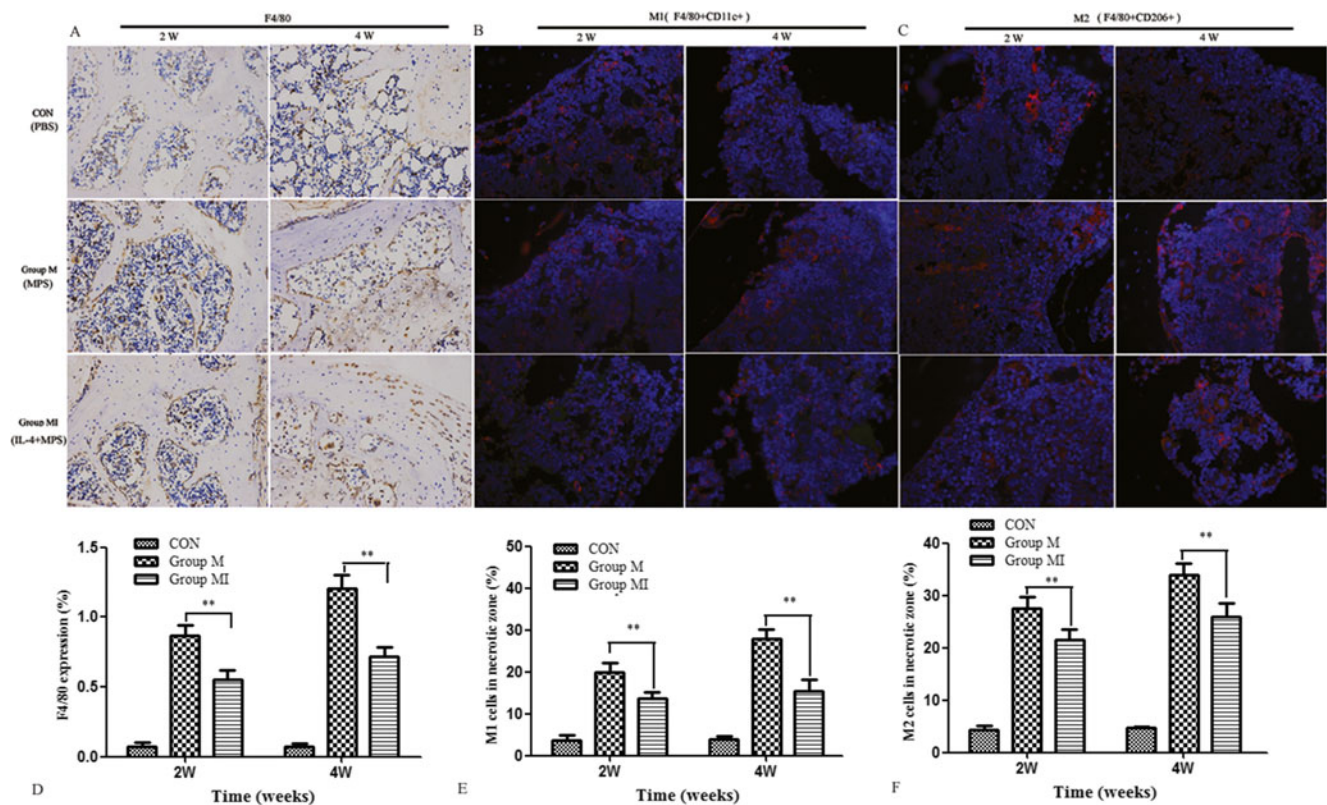

Fig. 4 Immunohistochemical and quantitative analyses of the protein expression of F4/80, CD11c, and CD206 in the necrotic bone tissue in groups treated with/without IL-4 intervention. a F4/80+-stained macrophages in the CON, M, and MI groups at weeks 2 and 4. b F4/80+CD11c+-stained macrophages in the CON, M, and MI groups at weeks 2 and 4. c F4/80+CD206+-stained macrophages in the CON, M,

and MI groups at weeks 2 and 4. d Statistical diagram showing the percentage of F4/80+ macrophages for different groups. e Cartogram showed the percentage of F4/80+CD11c+ macrophages at different groups. f Statistical diagram showed the percentage of F4/80+CD206+ macrophages of different groups. Data showed the mean ± SEM. **$P < 0.01$ vs. group M
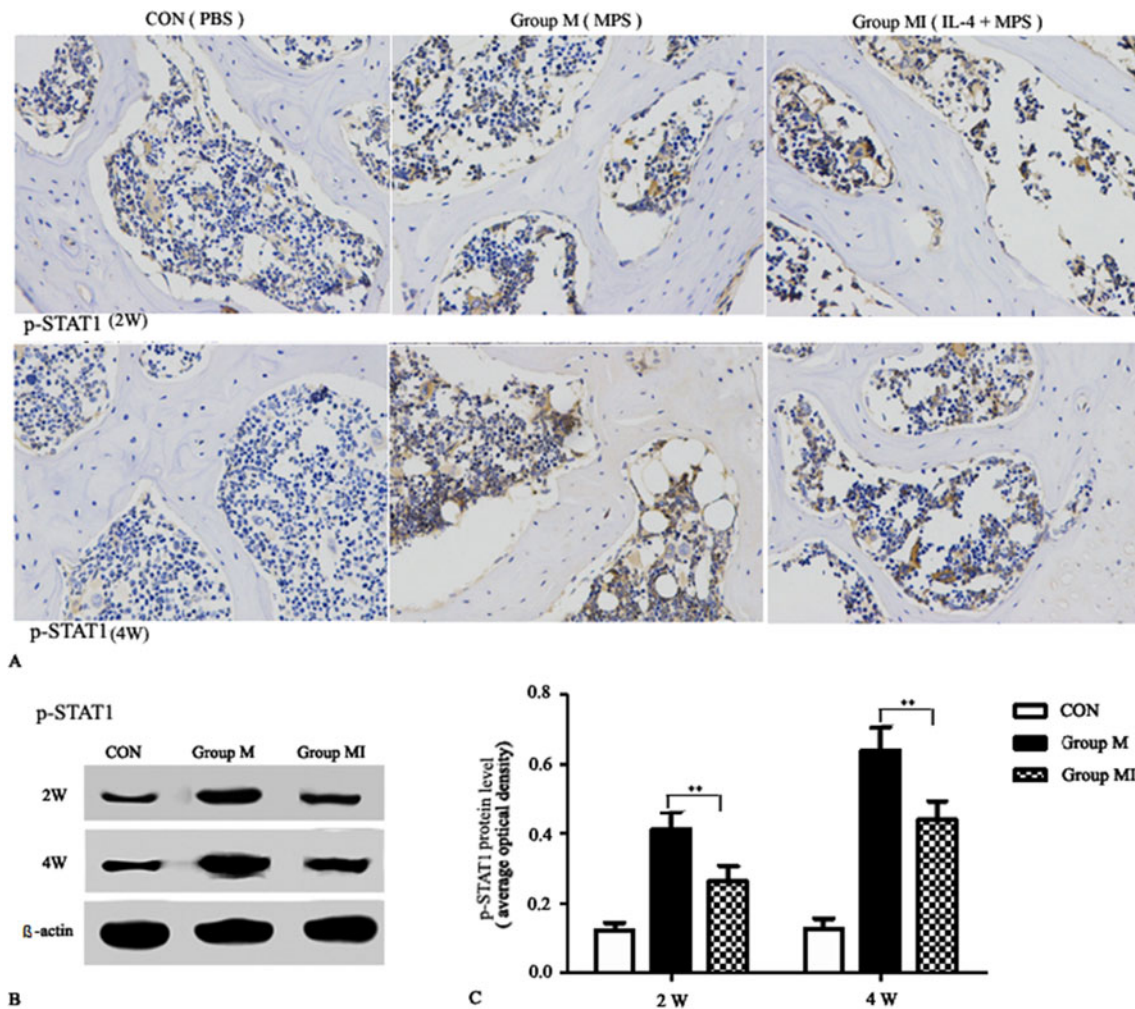
Fig. 5 p-STAT1 signal pathway during ON. **a** Immunohistochemical staining for p-STAT1 protein expression in the CON, M, and MI groups at weeks 2 and 4. **b** The expression of p-STAT1 protein was measured by Western blot analysis and immunoblotting. **c** Quantitative analysis for p-STAT1 protein expression measured by optical density and normalized to β-actin. Results were presented as mean $\pm$ SEM. **$P < 0.01$

Caspase-3 expression associated with development of ON

Caspase-3 has been reported to be the most frequently activated caspase protease in cell death process. The activity of caspase-3 protein was detected by immunofluorescence analysis. As shown by representative histological images in Fig. 6a, IL-4 treatment decreased the expression of caspase-3 protein in group MI at weeks 2 and 4, compared with that in group M. Minimal caspase-3 protein was detected in the CON group. Figure 6b, c demonstrates the increase of protein levels of caspase-3 during the process of ON, but the level of the signaling molecule of caspase-3 in group MI was significantly decreased compared to that in group M ($p < 0.05$). These results show that the caspase-3 signaling pathway plays an important role in the pathogenesis of ON, and IL-4 treatment can inhibit caspase-3 activity during ON.

TUNEL assay

Cell apoptosis is an important cause for death of osteocytes during the pathological progress of osteonecrosis. TUNEL assay is a common method for staining cells undergoing programmed cell death or apoptosis. In the control group, only a few apoptotic cells were observed, whereas a large number of apoptotic cells presented in the necrotic area in the experimental groups. In group M, the number of apoptotic cells increased significantly in the necrotic zone at weeks 2 and 4. Compared with group M, relatively lower number of TUNEL-positive osteocytes were observed in group MI after IL-4 treatment (Fig. 7). Thus, the findings indicated marked evidence of apoptotic osteocytes in ON, which could be alleviated by IL-4 administration.
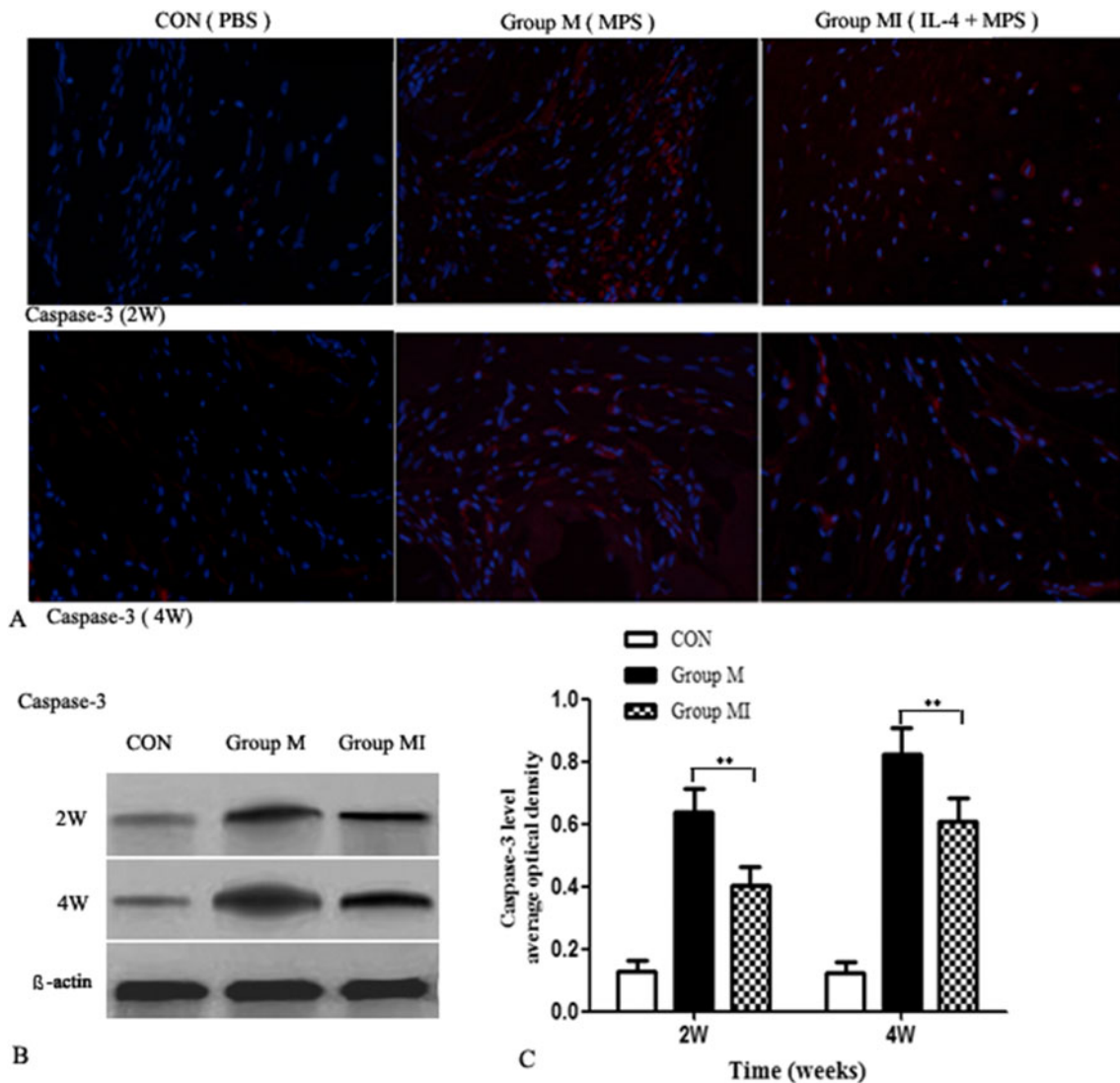
Fig. 6 Activity of Caspase-3 during ON. **a** Immunofluorescence staining for caspase-3 in the CON, M, and MI groups at weeks 2 and 4. **b** The expression of caspase-3 protein was measured by Western blot analysis and immunoblotting. **c** The amount of caspase-3 was measured by OD value and normalized to β-actin. Results were presented as mean ± SEM. **$P < 0.01$

Discussion

ON is a common complication with the use of systemic corticosteroids, which predominantly occurs in the femoral head, followed by the proximal humerus, knee, and ankle [9]. The pathological process of ON involves ischemic death of the bone and bone marrow, followed by a limited self-repair process. The study aimed to investigate the effects of IL-4 treatment on steroid-induced osteonecrosis and the appearance of M1/M2 macrophages as well as TNF-α and its downstream signals. The results showed that treatment with IL-4 was associated with a lower incidence of ON as seen by histological analysis. Additionally, the results revealed a significant decrease in the number of osteoclasts, expression of TNF-α protein, the number of F4/80-positive cells, F4/80 + CD11c + and F4/80 + CD206+ cells, and the amount of p-STAT1 protein in the bones of mice treated with a combination of MPS and IL-4 compared to those treated only with MPS. Moreover, IL-4 treatment decreased the number of apoptotic cells as measured by TUNEL and caspase-3 assays. Taken together, the results indicate the potential for IL-4 treatment to prevent steroid-induced osteonecrosis.

Previous studies indicated that glucocorticoid receptors (GR) are expressed in cartilage, osteoblasts, osteocytes, and osteoclasts in humans and mice [20–24]. Glucocorticoid (GC) excess could affect the growth, survival, and differentiation of osteoclasts in a direct and indirect manner to extend their life span, leading to early bone loss [25]. The survival and differentiation function of osteoclasts could be regulated by the factors produced by stromal and osteoblastic cells, such as
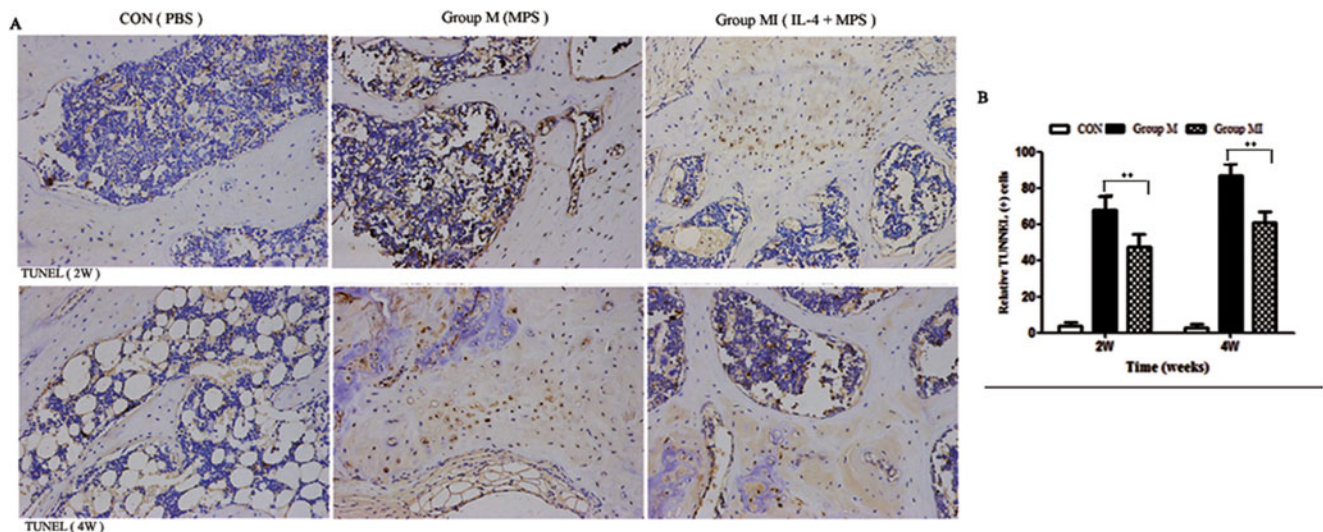
Fig. 7 TUNEL-positive staining indicating cell death during the progression of ON. **a** Representative histological sections of apoptosis as showed in the CON, M, and MI groups at weeks 2 and 4. **b** Statistical diagram showed the percentage of TUNEL-positive cells at different groups. Data showed the mean ± SEM. **P < 0.01 vs. group M

tumor necrosis factor (TNF-α). In addition to osteoclasts, macrophages have TRAP activity, which is related to the inflammatory response [26]. Inflammatory factors attract macrophages that continuously gather into the necrotic area; on the other hand, macrophages can themselves release inflammatory factors such as TNF-α, IL-6, and IL-12 [27]. During the progression of ON, necrotic bone marrow and bone cells are filled with hypertrophic adipocytes, which can release some inflammatory factors such as TNF-α and IL-6. TNF-α binds to the surface receptors of hypertrophic adipocytes, via the NF-kappa B (NFκB) and the MAPK signaling pathways, promoting the expression of pro-inflammatory factors and the disintegration of adipocytes [28]. Subsequently, a paracrine loop is established between adipocytes and macrophages through the secretion of TNF-α, aggravating inflammatory changes of adipose tissue through the upregulation of MCP-1 and TNF-α, and downregulation of adiponectin [29].

Therefore, steroid-induced osteonecrosis, characterized by an inflammatory process, is associated with the infiltration of macrophages into the necrotic area, which may contribute to an elevated inflammatory response by secreting a variety of pro-inflammatory factors. An M1-dominant response serves to clear debris and promotes the secretion of inflammatory cytokines and chemokines. The M1-driven pro-inflammatory phase is followed by a shift to a resolving M2 phenotype, which serves to restrain the inflammatory reaction and promotes differentiation of progenitor cells [30–32]. The anti-inflammatory property of M2 macrophages is correlated to the enhanced release of anti-inflammatory cytokines and reinforced phagocytosis potency of these macrophages compared to that of M1 macrophages [33, 34]. In addition, both clinical and animal experiments have confirmed that, during the

process of steroid-induced osteonecrosis, serum concentration of TNF-α is elevated, and the expression of TNF-α in the bone marrow of the femoral head increases significantly [35, 36]. In this study, the expression of TNF-α was weakened after IL-4 intervention, which might be useful for inhibiting the local inflammatory response and the accompanying necrotic progress. As the results show, during the progression of ON, predominant M1-polarized macrophages were observed in the necrotic site, which were switched to the M2-polarized macrophages by the treatment of IL-4, thus suppressing the inflammatory response and facilitating local bone repair.

More importantly, macrophages are a major target of GC, which exert their effects on the diversity of cells and apoptosis in the immune system [37]. An increasing number of studies have focused on the role of osteocyte apoptosis in steroid-induced osteonecrosis, which could induce a cumulative and irreparable defect and disrupt the mechanosensory function of the osteocyte-lacunar-canalicular system, resulting in collapse of the joint [38, 39]. Apoptotic cells need to be eliminated rapidly to prevent the release of tissue-damaging intracellular components that can induce inflammatory responses [40, 41]. From in vivo models and clinical studies, widespread apoptosis of osteoblasts and osteocytes was observed in the femurs of the patients with GC excess [42–44]. Weinstein et al. investigated the apoptotic phenomenon during the development of osteonecrosis, and their results indicated that osteocyte apoptosis was observed in glucocorticoid-induced ON but absent in post-traumatic ON [42]. Additionally, the study showed that osteocytic apoptosis was mainly detected proximal to the necrotic areas. Osteocyte/osteoblast apoptosis plays a determinant role in cortical bone loss and new bone formation in

steroid-induced osteonecrosis [45, 46]. The increased apoptosis of osteocytes and osteoblasts in repair tissue surrounding the necrotic area might be an important predictive factor for the collapse of the femoral head [47]. Failed repair processes might result in subchondral fracture and femoral head collapse by two methods: focal resorption of the necrotic trabeculae and excessive stress from pressure exerted on the femoral head [48]. Al-Dujaili et al. reported that apoptotic osteocytes targeted bone resorption by regulating osteoclast differentiation and accumulation [49]. Apoptosis is initiated in a variety of macrophages during osteoclast differentiation [50]. Thus, osteocytic apoptosis might be one of the main pathogenic features of steroid-induced osteonecrosis, accompanied by an increased number of recruited osteoclasts. Our findings are consistent with those reported in previous studies; the animals treated with IL-4 had less apoptotic cells in the necrotic zone at weeks 2 and 4 as measured by TUNEL.

Caspase-3 is a member of the cysteine-aspartic acid protease (caspase) family, which play a central role in the execution phase of cell apoptosis [51]. Caspase-3 is usually activated in apoptotic cells by both the extrinsic and intrinsic pathways [52, 53]. TNF-α is overproduced by adipocytes and macrophages during ON, which is involved in the induction of cell apoptosis. TNF-α acts as an apoptosis-inducing factor by activating caspase-3 through the receptor-mediated (Fas/FasL) or mitochondrial-dependent (Bax/Bcl-2) induction of apoptosis [54]. The binding of TNF-α to its receptor results in apoptosis in various cell types through JAKs or STATs [40, 55]. STAT family consists of seven family members, STAT1–4, 5A, 5B, and 6. STATs are required for the transduction of cytokine signals, and each STAT has its own responsive cytokines and specific signal [40]. Previous studies have reported that apoptosis depends on STAT1 through the expression of caspases, and STAT1-null cells are resistant to apoptosis induced by TNF-α [56, 57]. Our results showed that treatment with IL-4 could decrease TNF-α-induced osteocytic apoptosis by inhibiting the STAT1-caspase-3 signaling pathway.

In conclusion, steroid-induced ON partially caused the intensified inflammation, increased apoptosis of osteoblasts and osteocytes, and the prolonged lifespan of osteoclasts. IL-4 administration reduced the infiltration of M1 phenotypic macrophages and maintained the activation of M2 phenotypic macrophages, resulting in restriction of inflammation. TNF-α seemed to be relevant to the expression and phosphorylation of STAT1 and subsequent activation of caspase-3, and the apoptotic pathway could be inhibited by the intervention of IL-4.

Compliance with ethical standards

Conflicts of interest None.

References

1. Takano-Murakami R, Tokunaga K, Kondo N, Ito T, Kitahara H, Ito M, Endo N (2009) Glucocorticoid inhibits bone regeneration after osteonecrosis of the femoral head in aged female rats. Tohoku J Exp Med 217:51–58
2. McMahon RE, Bouquot JE, Glueck CJ, Spolnik KJ, Adams WR (2004) Osteonecrosis: a multifactorial etiology. J Oral Maxillofac Surg 62:904–905
3. Weinstein RS (2012) Glucocorticoid-induced osteonecrosis. Endocrine 41(2):183–190
4. Ross FP, Teitelbaum SL (2005) alphavbeta3 and macrophage colony-stimulating factor: partners in osteoclast biology. Immunol Rev 208:88–105
5. Gordon S (2007) The macrophage: past, present and future. Eur J Immunol 37(Suppl 1):S9–S17
6. Mantovani A, Sozzani S, Locati M, Allavena P, Sica A (2002) Macrophage polarization: tumor-associated macrophages as a paradigm for polarized M2 mononuclear phagocytes. Trends Immunol 23:549–555
7. Stout RD, Jiang C, Matta B, Tietzel I, Watkins SK, Suttles J (2005) Macrophages sequentially change their functional phenotype in response to changes in microenvironmental influences. J Immunol 175:342–349
8. Martinez FO, Helming L, Gordon S (2009) Alternative activation of macrophages: an immunologic functional perspective. Annu Rev Immunol 27:451–483
9. Nowicki P, Chaudhary H (2007) Total hip replacement in renal transplant patients. J Bone Joint Surg (Br) 89:1561–1566
10. Khallou-Laschet J, Varthaman A, Fornasa G, Compain C, Gaston AT, Clement M, Dussiot M, Levillain O, Graff-Dubois S, Nicoletti A, Caligiuri G (2010) Macrophage plasticity in experimental atherosclerosis. PLoS One 5:e8852
11. Frangogiannis NG (2012) Regulation of the inflammatory response in cardiac repair. Circ Res 110:159–173
12. Kharraz Y, Guerra J, Mann CJ, Serrano AL, Munoz-Canoves P (2013) Macrophage plasticity and the role of inflammation in skeletal muscle repair. Mediat Inflamm 491497
13. Thorp EB (2012) Contrasting inflammation resolution during atherosclerosis and post myocardial infarction at the level of monocyte/macrophage phagocytic clearance. Front Immunol 3:39
14. Villalta SA, Rinaldi C, Deng B, Liu G, Fedor B, Tidball JG (2011) Interleukin-10 reduces the pathology of mdx muscular dystrophy by deactivating M1 macrophages and modulating macrophage phenotype. Hum Mol Genet 20:790–805
15. Kigerl KA, Gensel JC, Ankeny DP, Alexander JK, Donnelly DJ, Popovich PG (2009) Identification of two distinct macrophage subsets with divergent effects causing either neurotoxicity or regeneration in the injured mouse spinal cord. J Neurosci 29:13435–13444
16. Brown BN, Ratner BD, Goodman SB, Amar S, Badylak SF (2012) Macrophage polarization: an opportunity for improved outcomes in biomaterials and regenerative medicine. Biomaterials 33:3792–3802
17. Nathan C, Ding A (2010) Nonresolving inflammation. Cell 140:871–882
18. Wu X, Xu W, Feng X, He Y, Liu X, Gao Y, Yang S, Shao Z, Yang C, Ye Z (2015) TNF-a mediated inflammatory macrophage polarization contributes to the pathogenesis of steroid-induced osteonecrosis in mice. Int J Immunopathol Pharmacol 28:351–361
19. Yamamoto T, Irisa T, Sugioka Y, Sueishi K (1997) Effects of pulse methylprednisolone on bone and marrow tissues: corticosteroid-induced osteonecrosis in rabbits. Arthritis Rheum 40:2055–2064
20. Chen WL, Lin CT, Yao CC, Huang YH, Chou YB, Yin HS, Hu FR (2006) In-vitro effects of dexamethasone on cellular proliferation,

apoptosis, and Na+-K+-ATPase activity of bovine corneal endothelial cells. Ocul Immunol Inflamm 14:215–223

21. Liesegang P, Romalo G, Sudmann M, Wolf L, Schweikert HU (1994) Human osteoblast-like cells contain specific, saturable, high-affinity glucocorticoid, androgen, estrogen, and 1 alpha,25-dihydroxycholecalciferol receptors. J Androl 15:194–199

22. Gu G, Hentunen TA, Nars M, Harkonen PL, Vaananen HK (2005) Estrogen protects primary osteocytes against glucocorticoid-induced apoptosis. Apoptosis 10:583–595

23. Dempster DW, Moonga BS, Stein LS, Horbert WR, Antakly T (1997) Glucocorticoids inhibit bone resorption by isolated rat osteoclasts by enhancing apoptosis. J Endocrinol 154:397–406

24. Silvestrini G, Mocetti P, Ballanti P, Di Grezia R, Bonucci E (1999) Cytochemical demonstration of the glucocorticoid receptor in skeletal cells of the rat. Endocr Res 25:117–128

25. Weinstein RS, Chen JR, Powers CC, Stewart SA, Landes RD, Bellido T, Jilka RL, Parfitt AM, Manolagas SC (2002) Promotion of osteoclast survival and antagonism of bisphosphonate-induced osteoclast apoptosis by glucocorticoids. J Clin Invest 109:1041–1048

26. Bune AJ, Hayman AR, Evans MJ, Cox TM (2001) Mice lacking tartrate-resistant acid phosphatase (Acp 5) have disordered macrophage inflammatory responses and reduced clearance of the pathogen, Staphylococcus aureus. Immunology 102:103–113

27. Miranville A, Herling AW, Biemer-Daub G, Voss MD (2010) Reversal of inflammation-induced impairment of glucose uptake in adipocytes by direct effect of CB1 antagonism on adipose tissue macrophages. Obesity (Silver Spring) 18:2247–2254

28. Suganami T, Ogawa Y (2010) Adipose tissue macrophages: their role in adipose tissue remodeling. J Leukoc Biol 88:33–39

29. Suganami T, Nishida J, Ogawa Y (2005) A paracrine loop between adipocytes and macrophages aggravates inflammatory changes: role of free fatty acids and tumor necrosis factor alpha. Arterioscler Thromb Vasc Biol 25:2062–2068

30. Tidball JG, Wehling-Henricks M (2007) Macrophages promote muscle membrane repair and muscle fibre growth and regeneration during modified muscle loading in mice in vivo. J Physiol 578:327–336

31. Li YP (2003) TNF-alpha is a mitogen in skeletal muscle. Am J Physiol Cell Physiol 285:C370–C376

32. Villalta SA, Deng B, Rinaldi C, Wehling-Henricks M, Tidball JG (2011) IFN-gamma promotes muscle damage in the mdx mouse model of Duchenne muscular dystrophy by suppressing M2 macrophage activation and inhibiting muscle cell proliferation. J Immunol 187:5419–5428

33. Porcheray F, Viaud S, Rimaniol AC, Leone C, Samah B, Dereuddre-Bosquet N, Dormont D, Gras G (2005) Macrophage activation switching: an asset for the resolution of inflammation. Clin Exp Immunol 142:481–489

34. Berger C, Hiestand P, Kindler-Baumann D, Rudin M, Rausch M (2006) Analysis of lesion development during acute inflammation and remission in a rat model of experimental autoimmune encephalomyelitis by visualization of macrophage infiltration, demyelination and blood-brain barrier damage. NMR Biomed 19:101–107

35. Okazaki S, Nishitani Y, Nagoya S, Kaya M, Yamashita T, Matsumoto H (2009) Femoral head osteonecrosis can be caused by disruption of the systemic immune response via the toll-like receptor 4 signalling pathway. Rheumatology (Oxford) 48:227–232

36. Scheper MA, Badros A, Chaisuparat R, Cullen KJ, Meiller TF (2009) Effect of zoledronic acid on oral fibroblasts and epithelial cells: a potential mechanism of bisphosphonate-associated osteonecrosis. Br J Haematol 144:667–676

37. Castro R, Zou J, Secombes CJ, Martin SA (2011) Cortisol modulates the induction of inflammatory gene expression in a rainbow trout macrophage cell line. Fish Shellfish Immunol 30:215–223

38. Weinstein RS (2011) Clinical practice. Glucocorticoid-induced bone disease. N Engl J Med 365:62–70

39. Weinstein RS (2012) Glucocorticoid-induced osteoporosis and osteonecrosis. Endocrinol Metab Clin N Am 41:595–611

40. Miyamoto T (2013) STATs and macrophage fusion. JAKSTAT 2: e24777

41. Yamamoto T, Irisa T, Sugioka Y, Sueishi K (1997) Effects of pulse methylprednisolone on bone and marrow tissues: corticosteroid-induced osteonecrosis in rabbits. Arthritis Rheum 40:2055–2064

42. Weinstein RS, Nicholas RW, Manolagas SC (2000) Apoptosis of osteocytes in glucocorticoid-induced osteonecrosis of the hip. J Clin Endocrinol Metab 85:2907–2912

43. Peled E, Bejar J, Zinman C, Boss JH (2007) Vasculature deprivation-induced osteonecrosis of rats' femoral heads associated with the formation of deep surface depressions. Arch Orthop Trauma Surg 127:369–374

44. Calder JD, Buttery L, Revell PA, Pearse M, Polak JM (2004) Apoptosis—a significant cause of bone cell death in osteonecrosis of the femoral head. J Bone Joint Surg (Br) 86:1209–1213

45. Silverman SL, Lane NE (2009) Glucocorticoid-induced osteoporosis. Curr Osteoporos Rep 7:23–26

46. Wu X, Yang S, Wang H, Meng C, Xu W, Duan D, Liu X (2013) G-CSF/SCF exert beneficial effects via anti-apoptosis in rabbits with steroid-associated osteonecrosis. Exp Mol Pathol 94:247–254

47. Mutijima E, De Maertelaer V, Deprez M, Malaise M, Hauzeur JP (2014) The apoptosis of osteoblasts and osteocytes in femoral head osteonecrosis: its specificity and its distribution. Clin Rheumatol 33:1791–1795

48. Glimcher MJ, Kenzora JE (1979) The biology of osteonecrosis of the human femoral head and its clinical implications. III. Discussion of the etiology and genesis of the pathological sequelae; comments on treatment. Clin Orthop Relat Res 140:273–312

49. Al-Dujaili SA, Lau E, Al-Dujaili H, Tsang K, Guenther A, You L (2011) Apoptotic osteocytes regulate osteoclast precursor recruitment and differentiation in vitro. J Cell Biochem 112:2412–2423

50. Song R, Liu X, Zhu J, Gao Q, Wang Q, Zhang J, Wang D, Cheng L, Hu D, Yuan Y, Gu J, Liu Z (2015) RhoV mediates apoptosis of RAW264.7 macrophages caused by osteoclast differentiation. Mol Med Rep 11:1153–1159

51. Alnemri ES, Livingston DJ, Nicholson DW, Salvesen G, Thornberry NA, Wong WW, Yuan J (1996) Human ICE/CED-3 protease nomenclature. Cell 87:171

52. Salvesen GS (2002) Caspases: opening the boxes and interpreting the arrows. Cell Death Differ 9:3–5

53. Ghavami S, Hashemi M, Ande SR, Yeganeh B, Xiao W, Eshraghi M, Bus CJ, Kadkhoda K, Wiechec E, Halayko AJ, Los M (2009) Apoptosis and cancer: mutations within caspase genes. J Med Genet 46:497–510

54. Woo SH, Park IC, Park MJ, Lee HC, Lee SJ, Chun YJ, Lee SH, Hong SI, Rhee CH (2002) Arsenic trioxide induces apoptosis through a reactive oxygen species-dependent pathway and loss of mitochondrial membrane potential in HeLa cells. Int J Oncol 21:57–63

55. Hsu H, Huang J, Shu HB, Baichwal V, Goeddel DV (1996) TNF-dependent recruitment of the protein kinase RIP to the TNF receptor-1 signaling complex. Immunity 4:387–396

56. Kumar A, Commane M, Flickinger TW, Horvath CM, Stark GR (1997) Defective TNF-alpha-induced apoptosis in STAT1-null cells due to low constitutive levels of caspases. Science 278:1630–1632

57. Nagata S, Golstein P (1995) The Fas death factor. Science 267: 1449–1456